

## iTRAQ-based proteomic analysis of adaptive response in the regenerating limb of the *Cynops orientalis* newt

XIAO-FANG GENG<sup>1,2,3</sup>, JIAN-LIN GUO<sup>2,3,4</sup>, XIA-YAN ZANG<sup>2,3,4</sup>, JING-YAN SUN<sup>2,3,4</sup>, PENG-FEI LI<sup>2,3,4</sup>, FU-CHUN ZHANG<sup>1\*</sup> and CUN-SHUAN XU<sup>2,3,4\*</sup>

<sup>1</sup>Xinjiang Key Laboratory of Biological Resources and Genetic Engineering, College of Life Science and Technology, Xinjiang University, Urumqi, <sup>2</sup>State Key Laboratory Cultivation Base for Cell Differentiation Regulation, Henan Normal University, Xinxiang, <sup>3</sup>Henan Engineering Laboratory for Bioengineering and Drug Development, Henan Normal University, Xinxiang and <sup>4</sup>College of Life Science, Henan Normal University, Xinxiang, China

**ABSTRACT** The newt has the powerful capacity to regenerate lost limbs following amputation, and represents an excellent model organism to study regenerative processes. However, the molecular basis of the adaptive response in the regenerating limb of the Chinese fire-bellied newt *Cynops orientalis* immediately after amputation remains unclear. To better understand the adaptive response immediately after limb amputation at the protein level, we used isobaric tags for relative and absolute quantitation (iTRAQ) coupled with LC-MS/MS methods to analyze changes in the proteome of the regenerating newt limb that occurred 2 h and 8 h after amputation. We identified 152 proteins with more than 1.5-fold change in expression compared to control. GO annotation analysis classified these proteins into several categories such as signaling, Ca<sup>2+</sup> binding and translocation, transcription and translation, immune response, cell death, cytoskeleton, metabolism, etc. Further ingenuity pathway analysis (IPA) showed that several signaling pathways were significantly changed at 2 h and 8 h after amputation, including EIF2 signaling, acute phase response signaling, tight junction signaling and calcium signaling, suggesting these pathways may be closely related to the adaptive response immediately after limb amputation. This work provides novel insights into understanding the molecular processes related to newt limb regeneration immediately after amputation, and a basis for further study of regenerative medicine.

**KEY WORDS:** *Cynops orientalis*, limb regeneration, proteomic, stress response, cell death

Among vertebrates, urodele salamanders possess remarkable capability to regenerate appendages from any level of amputation through blastema formation. Subsequently, blastema cells that morphologically resemble mesenchymal stem-like cells self-organize into the amputated limb parts (Bryant *et al.*, 2002, Nye *et al.*, 2003). Adult newt has already been used as an important model for the limb regeneration studies. The process of limb regeneration can be divided into three major phases: wound healing and dedifferentiation; blastema accumulation and blastema growth; differentiation and morphogenesis (Iten and Bryant, 1973). Following amputation, the wound surface is covered rapidly by epithelial cells, which form the wound epidermis at the end of the stump. More importantly, a specialized epithelium provides signals to the underlying cells of

the stump to dedifferentiate and/or maintain cell proliferation (Kumar *et al.*, 2007). After that, an avascular accumulation blastema was formed mainly by the dedifferentiation of the liberated cells at the amputated site through proteolysis of extracellular matrix (Brockes and Kumar, 2002, Morrison *et al.*, 2006). Once formed, the accumulation blastema undergoes proliferation, differentiation and morphogenesis to regenerate the limb (Vascotto *et al.*, 2005).

Analysis of the molecular basis of urodele limb regeneration is useful for understanding how we might achieve its ultimate goal of

---

*Abbreviations used in this paper:* iTRAQ, isobaric tags for relative and absolute quantitation; IPA, ingenuity pathway analysis.

---

\*Address correspondence to: Cunshuan Xu. State Key Laboratory Cultivation Base for Cell Differentiation Regulation, Henan Normal University, Xinxiang 453007, China. Tel.: +860373-3326001; Fax: +860373-3325410. E-mail: cellkeylab@126.com

Supplementary Material (two tables) for this paper is available at: <http://dx.doi.org/10.1387/ijdb.150363cx>

Accepted: 5 November 2015.

stimulating limb regeneration of humans. More global analyses have recently been conducted using microarrays and high-throughput sequencing to compare transcriptional profiles of regenerating versus intact limb tissues, or to compare blastemas of regeneration-competent versus regeneration-deficient limbs (Grow *et al.*, 2006, Monaghan *et al.*, 2009, Wu *et al.*, 2013).

Recently, a number of studies have been carried out on protein separation and identification in regenerating urodele limb using gel-based proteomic method (Geng *et al.*, 2014, Tsonis, 1993, Tsonis *et al.*, 1992). Besides, Rao *et al.*, (Rao *et al.*, 2009) utilized a label-free LC-MS/MS quantitative approach to analyze blastema formation in regenerating axolotl hind limbs after amputation, and reported that the amputated urodele limb used a combination of mechanisms to regulate apoptosis during blastema formation that might be essential for dedifferentiation. Following amputation, there is a wide range of signals that induce proteolysis of extracellular matrix and promote liberation of cells from their initial tissue organization. To contradict this stress, cells use a variety of mechanisms to prevent apoptosis, including the up-regulation of anti-apoptotic pathways, metabolism reduction, and the initiation of unfolded protein response (Rao *et al.*, 2009). Although molecular details about the process of limb regeneration in amphibian have been uncovered, a specific event that takes place in regenerating newt limb immediately after amputation needs to be further studied.

In the present study, an isobaric tag for relative and absolute quantitation (iTRAQ) labeling combined with LC-MS/MS was utilized to determine the proteome changes of the regenerating newt limb immediately after amputation. The results revealed that 152 proteins showed more than 1.5-fold change in expression at 2 h and 8 h after amputation compared to control. Functional annotation found that these proteins were mainly involved in several functional categories including signaling, Ca<sup>2+</sup> binding and translocation, apoptosis and metabolism. Further IPA analysis showed that several signaling pathways including acute phase response signaling and calcium signaling maybe closely related to the adaptive response immediately after limb amputation. This work provides novel insights into understanding the molecular process related to newt limb regeneration.

## Results

### *Proteome alterations in the regenerating newt limbs immediately after amputation*

To identify proteins associated with the adaptive response in the regenerating newt limbs immediately after amputation, iTRAQ was employed to assess proteome changes at 2 h and 8 h following amputation, and Q-Exactive mass spectrometer was used to obtain better coverage of tissue proteome. The mass data was searched against the SwissProt database using Mascot 2.2 search engine. The peptide FDR  $\leq 0.01$  and each protein with at least 2 unique peptides were utilized to filter out the data, and 1787 proteins were identified (Supplementary table 1). The protein mass distribution mainly concentrated in 10–100 kDa which made up 87.01% of the proteins. The proteins with 2–5 peptides, 6–10 peptides, and above 11 peptides comprised 1067, 410 and 310, respectively (Fig. 1A). Protein sequence coverage with below 10%, 10–20%, 20–30%, 30–40%, 40–50%, and 50–100% variation accounted for 22.38%, 25.24%, 18.69%, 14.05%, 10.24% and 9.40% coverage, respectively (Fig. 1B).

Proteins that showed greater than 1.5-fold change in relative abundance were defined as significantly changed proteins. In total, 152 proteins were found to be differentially expressed at 2 h and 8 h after amputation as compared to control group, of which 91 proteins were up-regulated and 61 proteins down-regulated. Later on, to understand the expression trend as a whole, clustering was used in this study. Ratio values of 152 significantly changed proteins were log (base 2) transformed, and then hierarchical clustering was performed using Cluster 3.0 and TreeView software. A global intensity map of the differentially expressed proteins is shown in Fig. 2.

### *Functional categories of the significantly changed proteins in the regenerating newt limbs immediately after amputation*

Fig. 3 stratifies the proteins according to biological process and molecular function. Among the 152 differentially expressed proteins, 129 proteins were categorized into seven groups according to their functional properties: (i) signaling; (ii) Ca<sup>2+</sup> binding and

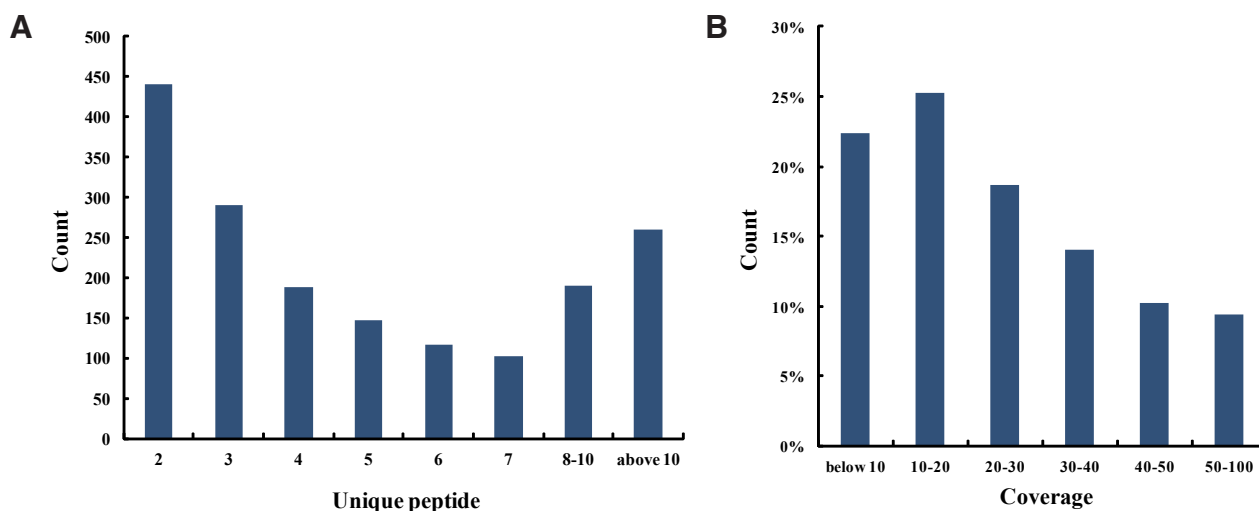


**Fig. 1.** The unique peptides and the sequence coverage of the identified proteins. (A) The number of the identified proteins with different unique peptides. (B) The percent of the identified proteins with different sequence coverage.

translocation; (iii) transcription and translation; (iv) cytoskeleton; (v) immune response and cell death; (vi) carbohydrate, lipid, and energy metabolism; and (vii) amino acid and purine metabolism (Table 1). Below, we describe the results for each of the biological categories in order.

8 differentially expressed proteins belong to proteins associated with signaling. Among them, RAN GTPase activating protein 1, SPARC-like protein 1, RAC-beta serine/threonine-protein kinase and cytoplasmic FMR1-interacting protein 1 were up-regulated immediately after amputation.

14 differentially expressed proteins belong to proteins associated with Ca<sup>2+</sup> binding and translocation, and the number of up-regulated proteins was significantly more than that of down-regulated proteins. These proteins included solute carrier family 25 members, S100 calcium binding protein A10, sarcoendoplasmic reticulum calcium ATPase, tricarboxylate transport protein, etc.

21 differentially expressed proteins were involved in transcription and translation. We found that most of the proteins related to translation were significantly down-regulated, especially at 2 h, including ribosomal proteins, eukaryotic translation initiation factors and elongation factors.

15 differentially expressed proteins belong to proteins associated with cytoskeleton and extracellular matrix. Among them, seven proteins were up-regulated at 2 h and 8 h after amputation, including myosins, tubulins, and regulator of microtubule dynamics protein 1.

18 differentially expressed proteins were involved in immune response and cell death. We found that the number of up-regulated proteins was significantly more than that of down-regulated proteins. These proteins including complement component C3, stress-70 protein, heat shock protein 5, superoxide dismutase [Cu-Zn], etc.

53 differentially expressed proteins were found to participate in metabolism. Among them, 36 proteins were involved in carbohydrate, lipid, and energy metabolism. Interestingly, the number of the up-regulated proteins was 2-fold lower than that of the down-regulated proteins at 2 h, and the number of the up-regulated proteins was 2-fold higher than that of the down-regulated proteins at 8 h. More importantly, most of the proteins showed significantly up-regulated at 8 h after amputation, including proteins related to glycolysis (i.e. phosphoglycerate kinase, glycerol-3-phosphate dehydrogenase 1), tricarboxylic acid cycle (i.e. 2-oxoglutarate dehydrogenase, pyruvate dehydrogenase E1 component, isocitrate dehydrogenase), electron transport chain (i.e. NADH dehydrogenase [ubiquinone] iron-sulfur protein 2), and fatty acid oxidation (i.e. acyl-Coenzyme A dehydrogenase, very long-chain specific acyl-CoA dehydrogenase, hydroxyacyl-Coenzyme A dehydrogenase). 17 proteins were involved in amino acid and purine metabolism. Similar to the expression pattern of carbohydrate, lipid, and energy metabolism, most of the proteins showed significantly up-regulated at 8 h after amputation, including proteins associated with amino acid metabolism (i.e. aspartate aminotransferase, 4-aminobutyrate aminotransferase, alanine aminotransferase) and purine metabolism (i.e. purine nucleoside

phosphorylase, nucleoside diphosphate kinase).

### Modulation of various signaling pathways at the very early phase of newt limb regeneration

To further clarify which signaling pathways play important roles at the very early phase of newt limb regeneration, IPA analysis was carried out to connect the differentially expressed proteins with canonical pathways. The significance of a canonical pathway was calculated by a Benjamini-Hochberg corrected Fischer's exact test. The pathway analysis results showed that several signaling

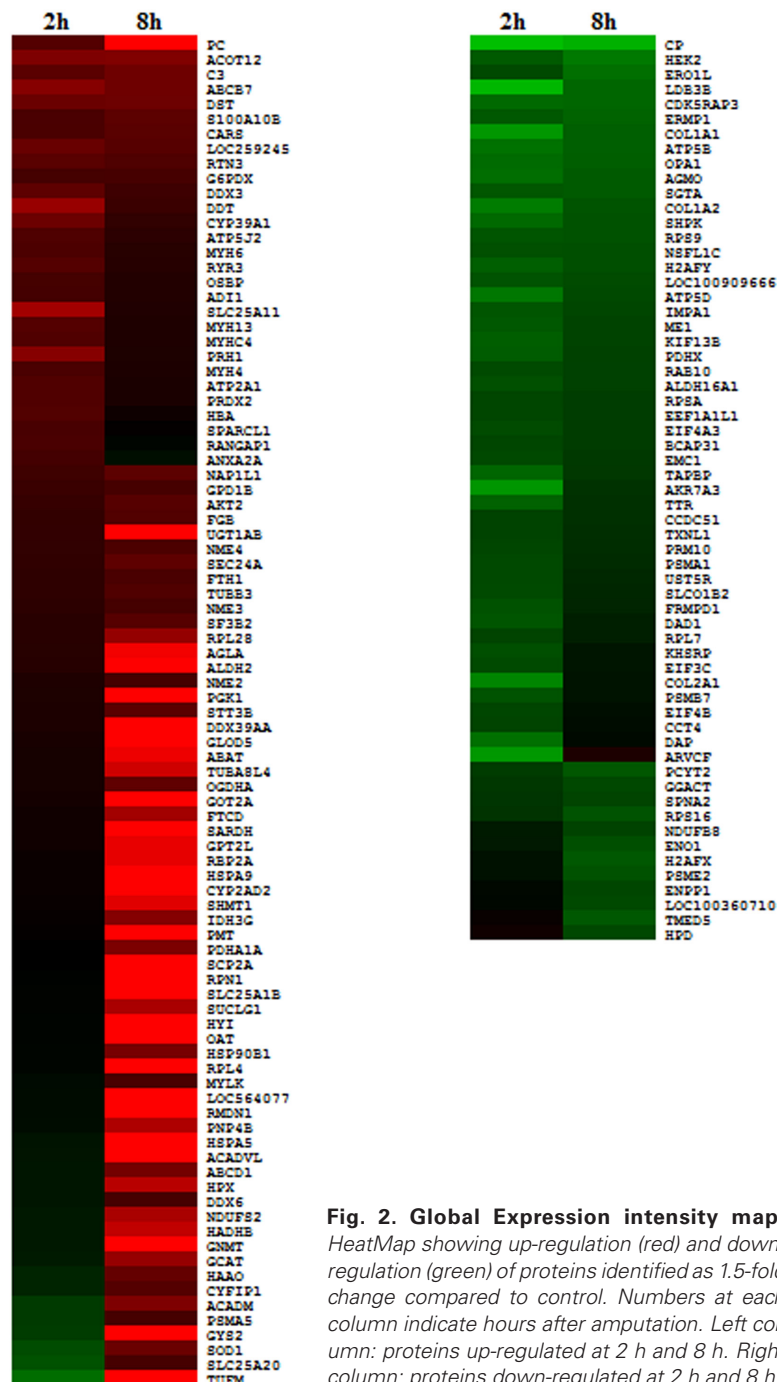


**Fig. 2. Global Expression intensity map.** HeatMap showing up-regulation (red) and down-regulation (green) of proteins identified as 1.5-fold change compared to control. Numbers at each column indicate hours after amputation. Left column: proteins up-regulated at 2 h and 8 h. Right column: proteins down-regulated at 2 h and 8 h.

TABLE 1

## PROTEOME ALTERATIONS IN THE REGENERATING NEWT LIMB IMMEDIATELY AFTER AMPUTATION

Protein name	Genes	MW [kDa]	pI	Coverage	Unique Peptides	2h/0h	8h/0h
<b>Signaling</b>							
RAN GTPase activating protein 1	RANGAP1	46.4	4.6	4.2	2	1.57	0.97
SPARC-like protein 1	SPARCL1	29.7	5.0	14.2	2	1.56	1.03
Annexin A2	ANXA2	38.1	7.7	19.6	5	1.51	0.91
Cytoplasmic FMR1-interacting protein 1	CYFIP1	144.8	6.9	2.6	3	0.80	1.68
B-cell receptor-associated protein 31	BCAP31	28.0	8.6	8.5	2	0.66	0.69
ERO1-like protein alpha	ERO1L	53.9	5.9	5.2	2	0.64	0.51
Inositol monophosphatase 1	IMPA1	30.5	5.3	15.9	3	0.60	0.66
RAB10, member RAS oncogene family	RAB10	22.5	8.4	22.5	2	0.64	0.68
<b>Ca<sup>2+</sup> binding and translocation</b>							
ATP-binding cassette sub-family B member 7	ABCB7	73.7	9.1	3.3	2	2.26	1.96
S100 calcium binding protein A10	S100A10	11.1	5.5	24.0	2	1.57	1.76
Dystonin	DST	607.8	5.8	0.4	2	1.91	1.94
Ryanodine receptor 3	RYR3	548.4	6.0	0.5	2	1.67	1.26
Sarcoendoplasmic reticulum calcium ATPase	ATP2A1	108.7	5.2	20.5	6	1.63	1.18
Oxysterol-binding protein	OSBP	84.9	7.3	3.6	3	1.52	1.24
Hemoglobin subunit alpha	HBA	15.7	7.7	21.8	2	1.66	1.10
Solute carrier family 25 member 11	SLC25A11	33.8	9.8	15.3	2	2.67	1.22
Solute carrier family 22 member 6	SLC22A6	48.6	7.0	26.6	7	0.97	13.56
Tricarboxylate transport protein, mitochondrial	SLC25A1	45.1	9.8	21.7	5	0.98	9.66
Solute carrier family 25 member 20	SLC25A20	32.8	9.5	13.3	2	0.61	1.54
Ceruloplasmin	CP	124.3	6.9	6.9	6	0.32	0.34
T-complex protein 1 subunit delta	CCT4	58.1	8.0	22.8	5	0.66	0.93
Transmembrane emp24 domain-containing protein 5	TMED5	26.1	4.8	14.4	3	1.06	0.59
<b>Transcription and translation</b>							
Cysteine--tRNA ligase, cytoplasmic	CARS	74.6	6.4	6.1	3	1.58	1.71
DEAD (Asp-Glu-Ala-Asp) box polypeptide 3	DDX3X	78.3	8.3	13.0	2	1.78	1.46
ATP-dependent RNA helicase DDX39A	DDX39A	48.9	5.6	26.9	3	1.19	6.63
Ribosomal protein L4	RPL4	42.5	11.1	27.2	9	0.97	6.36
Ribophorin-1	RPN1	67.6	6.7	22.7	10	0.99	5.12
60S ribosomal protein L28	RPL28	15.6	12.1	20.3	3	1.28	2.45
Splicing factor 3B subunit 2	SF3B2	98.3	5.5	2.2	2	1.28	1.68
Probable ATP-dependent RNA helicase ddx6	DDX6	54.2	8.7	12.0	4	0.88	1.54
Nucleosome assembly protein 1, like 1	NAP1L1	44.4	4.5	17.4	2	1.47	1.76
40S ribosomal protein S9	RPS9	22.6	10.7	40.2	4	0.60	0.61
Ribosomal protein S2	RPS2	27.2	9.6	35.2	3	0.96	0.64
Ribosomal protein S16	RPS16	16.3	10.1	39.7	2	0.73	0.61
Elongation factor Tu	TUFM	49.2	6.9	17.2	5	0.52	6.44
60S ribosomal protein L7	RPL7	30.3	10.9	31.9	7	0.66	0.83
Eukaryotic translation initiation factor 4B	EIF4B	69.0	5.8	9.5	5	0.66	0.91
40S ribosomal protein SA	RPSA	32.8	4.9	35.6	2	0.66	0.69
Elongation factor 1-alpha	EEF1A1	50.0	8.9	49.8	5	0.65	0.69
ER membrane protein complex subunit 1	EMC1	111.1	7.3	4.9	5	0.64	0.71
Eukaryotic translation initiation factor 3 subunit C	EIF3C	105.4	5.8	6.3	2	0.64	0.88
Eukaryotic initiation factor 4A-III	EIF4A3	46.4	6.7	12.8	2	0.63	0.69
Far upstream element-binding protein 2	KHSRP	74.2	6.9	10.1	5	0.62	0.88
<b>Cytoskeleton and extracellular matrix</b>							
Myosin-13	MYH13	208.8	5.6	21.5	5	1.68	1.21
Myosin-6	MYH6	223.4	5.7	30.6	3	1.58	1.27
Myosin-4	MYH4	222.7	5.7	30.5	4	1.56	1.18
Regulator of microtubule dynamics protein 1	RMDN1	34.1	8.0	10.9	3	0.93	5.46
Tubulin alpha 6	TUBA1C	50.0	5.1	60.0	2	1.15	3.50
Tubulin beta-3 chain	TUBB3	50.4	4.9	41.6	2	1.33	1.63
Myosin light chain kinase, smooth muscle	MYLK	212.9	6.0	1.5	2	0.94	1.58
Fibrinogen beta chain	FGB	54.2	7.8	13.4	5	1.37	1.65
Kinesin-like protein	KIF13B	195.0	5.6	2.3	3	0.56	0.67
LIM domain binding 3	LDB3	31.5	9.1	14.4	2	0.33	0.53
Collagen alpha-1(I) chain	COL1A1	137.5	5.6	21.0	24	0.40	0.56
Collagen type I alpha 2	COL1A2	127.7	8.7	5.7	6	0.47	0.60
Alpha1 type II collagen	COL2A1	135.0	7.8	5.2	6	0.45	0.89
FERM domain containing-1	FRMPD1	59.7	6.3	6.6	4	0.61	0.80
Alpha II-spectrin	SPTAN1	284.8	5.2	22.7	12	0.73	0.66
<b>Immune response and cell death</b>							
D-dopachrome decarboxylase	DDT	12.9	7.1	25.4	2	2.50	1.42
Complement component C3	C3	45.6	7.1	13.6	4	1.73	1.96
Reticulon 3	RTN3	24.5	9.0	13.1	2	1.72	1.62
Peroxiredoxin-2	PRDX2	21.8	5.6	23.7	5	1.63	1.18
RAC-beta serine/threonine-protein kinase	AKT2	55.5	6.4	3.3	2	1.39	1.69
Stress-70 protein, mitochondrial	HSPA9	73.9	7.1	34.9	5	1.06	7.77
Heat shock protein 5	HSPA5	71.9	5.1	49.7	6	0.89	6.01
Hemopexin	HPX	51.0	6.6	30.0	12	0.88	3.06
Chaperone protein GP96	HSP90B1	91.2	4.9	37.5	14	0.97	2.07
Superoxide dismutase [Cu-Zn]	SOD1	15.9	6.6	64.9	8	0.63	1.91
Ferritin heavy chain	FTH1	21.1	6.3	39.0	5	1.34	1.57
Proteasome subunit alpha type	PSMA5	26.4	4.8	30.3	2	0.70	1.54
Proteasome activator complex subunit 2	PSME2	26.8	5.7	28.2	2	0.90	0.61
Dynamamin-like 120 kDa protein, mitochondrial	OPA1	111.2	7.5	10.7	5	0.52	0.56
Proteasome subunit alpha type-1	PSMA1	29.5	6.6	38.0	3	0.64	0.77
Oligosaccharyl transferase subunit DAD1	DAD1	12.5	7.1	19.5	2	0.59	0.83
Proteasome subunit beta type-7	PSMB7	29.9	8.0	13.7	3	0.60	0.89
Death-associated protein 1	DAP	11.2	9.6	15.7	2	0.50	0.94

TABLE 1 (CONTINUED)

## PROTEOME ALTERATIONS IN THE REGENERATING NEWT LIMB IMMEDIATELY AFTER AMPUTATION

Protein name	Genes	MW [kDa]	pI	Coverage	Unique Peptides	2h/0h	8h/0h
<b>Carbohydrate, lipid, and energy metabolism</b>							
Acyl-coenzyme A thioesterase 12	ACOT12	62.0	7.2	4.9	2	2.16	2.18
Pyruvate carboxylase	PC	129.9	6.9	42.5	21	1.66	10.64
24-hydroxycholesterol 7- $\alpha$ -hydroxylase	CYP39A1	48.0	9.1	7.6	3	1.93	1.35
ATP synthase subunit f, mitochondrial	ATP5J2	10.4	10.0	23.9	2	1.62	1.31
Glucose-6-phosphate 1-dehydrogenase	G6PD	57.7	8.0	5.6	2	1.52	1.54
Very long-chain specific acyl-CoA dehydrogenase	ACADVL	71.0	8.4	13.8	7	0.88	14.97
Phosphoglycerate kinase	PGK1	44.7	6.9	53.2	11	1.20	12.44
Glycogen synthase 2	GYS2	80.5	6.6	5.0	3	0.69	7.88
Aldehyde dehydrogenase 2 family	ALDH2	56.5	6.3	45.5	6	1.26	6.75
Hydroxypyruvate isomerase	HYI	31.0	5.6	10.5	3	0.97	6.59
Sterol carrier protein 2	SCP2	57.9	7.4	20.1	6	1.01	4.73
Cellular retinol-binding protein type II	RBP2	15.8	6.5	37.0	4	1.07	4.01
Hydroxyacyl-Coenzyme A dehydrogenase beta subunit	HADHB	49.9	9.2	27.6	2	0.86	3.22
Succinyl-CoA ligase [ADP/GDP-forming] subunit alpha, mitochondrial	SUCLG1	34.2	9.1	42.3	6	0.98	2.80
NADH dehydrogenase [ubiquinone] iron-sulfur protein 2	NDUFS2	52.7	6.8	14.4	2	0.87	2.78
Isocitrate dehydrogenase [NAD] subunit, mitochondrial	IDH3G	42.7	8.9	10.2	2	1.04	2.25
Acyl-Coenzyme A dehydrogenase	ACADM	46.1	8.0	27.1	7	0.70	2.16
Pyruvate dehydrogenase E1 component subunit alpha	PDHA1	43.7	8.0	19.6	4	1.01	2.12
ATP-binding cassette, sub-family D (ALD), member 1	ABCD1	81.9	8.5	4.3	2	0.88	2.02
2-oxoglutarate dehydrogenase, mitochondrial	OGDH	115.6	6.9	15.1	8	1.15	1.79
Protein Sec24a	SEC24A	118.8	7.6	3.1	3	1.34	1.79
Oligosaccharyl transferase subunit STT3B	STT3B	93.4	9.4	8.2	6	1.19	1.74
Glycerol-3-phosphate dehydrogenase 1	GPD1	38.2	6.8	53.1	12	1.42	1.54
NADH dehydrogenase (Ubiquinone) 1 beta subcomplex 8	NDUFB8	21.9	6.0	12.4	2	0.85	0.67
Ectonucleotide pyrophosphatase/phosphodiesterase 1	ENPP1	102.8	6.6	10.4	7	0.95	0.65
Enolase	ENO1	17.1	9.0	37.9	4	0.86	0.62
Ethanolamine-phosphate cytidyltransferase	PCYT2	45.2	6.7	14.1	5	0.70	0.59
Aldehyde dehydrogenase family 16 member A1	ALDH16A1	85.4	6.2	3.7	2	0.61	0.68
Malic enzyme	ME1	64.5	7.3	20.2	9	0.59	0.66
Pyruvate dehydrogenase protein X component	PDHX	40.9	8.7	9.0	3	0.57	0.67
Transthyretin	TTR	15.7	6.2	17.0	2	0.55	0.75
Carbohydrate kinase-like	SHPK	50.6	5.9	8.7	3	0.53	0.61
Alkylglycerol monoxygenase	AGMO	51.7	7.6	5.8	2	0.51	0.58
ATP synthase subunit beta	ATP5B	46.1	5.1	44.0	2	0.50	0.56
ATP synthase subunit delta, mitochondrial	ATP5D	17.6	5.2	13.7	2	0.49	0.64
Aflatoxin B1 aldehyde reductase member 3	AKR7A3	36.5	6.7	16.7	4	0.40	0.74
1,2-dihydroxy-3-keto-5-methylthiopentene dioxygenase	ADI1	21.4	5.4	21.2	3	1.51	1.23
<b>Amino acid and purine metabolism</b>							
Aspartate aminotransferase	GOT2	47.6	9.2	45.3	14	1.14	19.45
Glycine N-methyltransferase	GNMT	33.2	6.9	33.3	6	0.86	7.14
Sarcosine dehydrogenase, mitochondrial	SARDH	102.8	7.2	19.4	4	1.11	5.71
4-aminobutyrate aminotransferase	ABAT	55.7	7.7	35.6	12	1.15	4.23
Alanine aminotransferase 2	GPT2	61.1	8.3	46.5	14	1.11	4.07
Serine hydroxymethyltransferase	SHMT1	53.3	7.9	39.1	12	1.05	3.90
Purine nucleoside phosphorylase	PNP	33.8	7.0	25.0	4	0.92	2.88
Formimidoyltransferase-cyclodeaminase	FTCD	60.3	7.0	40.0	18	1.11	2.68
2-amino-3-ketobutyrate coenzyme A ligase	GCAT	49.6	8.1	30.4	11	0.85	2.50
3-hydroxyanthranilate 3,4-dioxygenase	HAAO	33.2	5.7	31.7	8	0.80	1.85
Nucleoside diphosphate kinase, mitochondrial	NME4	21.2	9.7	46.3	8	1.35	1.59
Nucleoside diphosphate kinase B	NME2	17.3	7.4	67.8	3	1.20	1.54
Nucleoside diphosphate kinase DR-nm23	NME3	19.1	6.3	28.4	3	1.31	1.52
Gamma-glutamylaminocyclotransferase	GGACT	16.9	6.5	20.1	2	0.72	0.65
4-hydroxyphenylpyruvate dioxygenase	HPD	45.2	6.8	57.9	2	1.11	0.64
Endoplasmic reticulum metalloproteinase 1	ERMP1	99.9	7.5	3.7	3	0.58	0.55

pathways were significantly changed at 2 h and 8 h after amputation, including EIF2 signaling, acute phase response signaling, tight junction signaling, protein ubiquitination pathway, calcium signaling, endoplasmic reticulum stress pathway and PI3K/AKT signaling, indicating that these pathways play predominant roles at the very early phase of newt limb regeneration (Fig. 4). A detailed pathway enrichment of the differentially expressed proteins at the very early phase of newt limb regeneration was provided in Supplementary Table 2.

## Discussion

iTRAQ coupled with LC-MS/MS method is rapid and more sensitive than many other proteomic methods, and increases the protein dynamic range of threefold to fourfold compared to two-dimensional gel electrophoresis. Therefore, we used this method to examine the protein expression changes in the regenerating newt

limbs immediately after amputation, and found that 152 proteins were significantly altered at 2 h and 8 h after amputation. Based on these results, we could ratiocinate that the fluctuation in protein level immediately after amputation was associated with adaptive response in newt limb regeneration, such as immune response, cell death and metabolism.

### Signaling, $Ca^{2+}$ binding and translocation

It has been reported that limb amputation causes a major increase in the level of cytosolic  $Ca^{2+}$ , and calcium signaling is essential for newt limb regeneration in the axolotl (Globus *et al.*, 1987, Rao *et al.*, 2009). Consistent with this result, we also found that calcium signaling was significantly changed at the very early phase of newt limb regeneration. In addition,  $Ca^{2+}$ -binding protein S100A10 was up-regulated at 2 h and 8 h after amputation of the newt limb, in harmony with studies showing that the expression level of several S100 family  $Ca^{2+}$ -binding proteins were enhanced in the

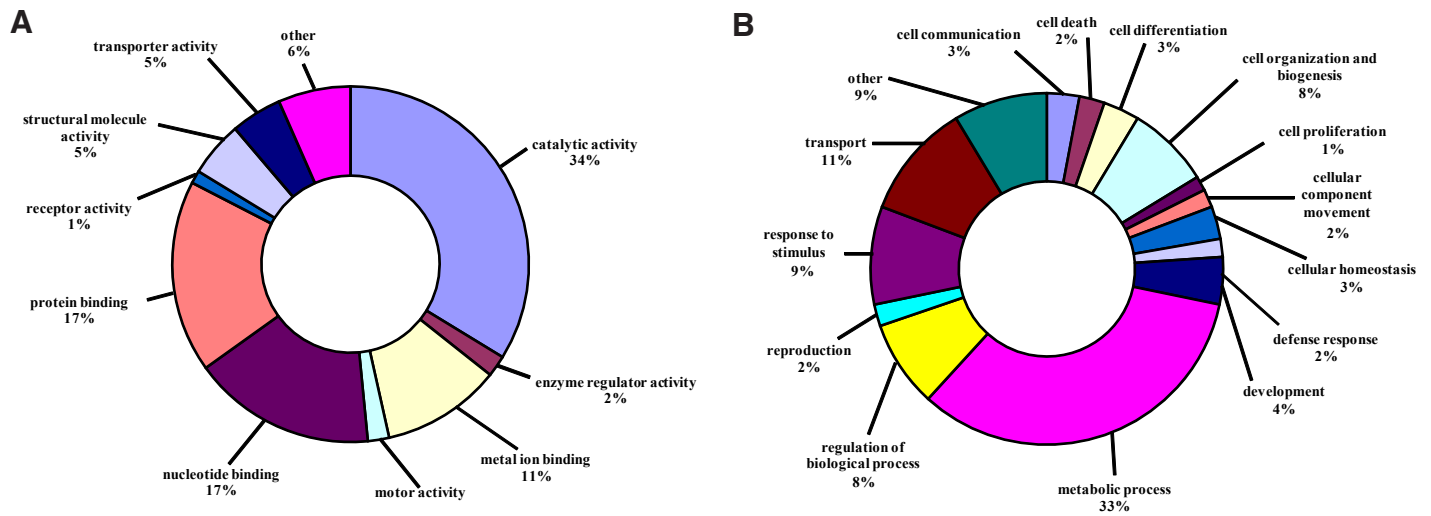


**Fig. 3. Functional and cellular categorization of proteins.** Pie charts showing categories of 152 proteins according to (A) molecular function and (B) biological process.

regenerating ear tissue of MRL/Mpj-Fas mice and in regeneration-competent stage 53 *Xenopus* limb buds (Caldwell *et al.*, 2008, King *et al.*, 2009). Moreover, other  $Ca^{2+}$ -binding proteins such as ryanodine receptor and ATP2A1 were up-regulated. Ryanodine receptor is involved in skeletal muscle contraction by releasing calcium from the sarcoplasmic reticulum followed by depolarization of T-tubules (Sei *et al.*, 1999). ATP2A1 is intracellular pump located in the sarcoplasmic or endoplasmic reticula of muscle cells and is also involved in muscle contraction. These results suggest that calcium signaling is a key event at the very early phase of newt limb regeneration.

Annexins, calcium-dependent phospholipid-binding proteins with various biological processes, were detected in the regenerating limbs of both axolotl and froglet, and might be important for histolysis during limb regeneration (Menea *et al.*, 1999, Rao *et al.*, 2014). In the present study, the protein ubiquitination pathway essential for histolysis was significantly changed at the very early phase of newt limb regeneration. In addition, annexin 2 was found to be up-regulated at 2 h after amputation, consistent with the finding that the expression level of annexin 2 was significantly increased in the regenerating amphibian limbs (King *et al.*, 2009, Rao *et al.*, 2009), suggesting that annexin 2 plays an important role in newt limb regeneration.

Rab family GTPases play a critical role in regulating intracellular vesicle trafficking of proteins (Takai *et al.*, 2001). Several Rab family GTPases and their activators and exchangers were found to be differentially regulated in the regenerating axolotl limb after amputation (Rao *et al.*, 2009). In this study, RAB10 belonging to the RAS superfamily of small GTPases was differentially expressed at 2 h after amputation of newt limb. In addition, RANGAP1 was critically involved in smooth muscle cell differentiation, proliferation and migration following vascular injury (Vorpahl *et al.*, 2014), and was found to be up-regulated at 2 h after amputation of newt limb. These results indicate that proteins associated with  $Ca^{2+}$  binding and translocation are predominant during newt limb regeneration.

### Transcription and translation

Studies have indicated that both RNA and protein synthesis are

enhanced during blastema formation of limb regeneration (Morzlock and Stocum, 1971, Tsonis *et al.*, 1992). DDX39A belonging a member of the DEAD box protein family, was up-regulated at the very early phase of newt limb regeneration, and implicated in a number of cellular processes such as translation initiation and the assembly of ribosome and spliceosome. Study has reported that tRNA aminoacylation-related protein TARSL2 was up-regulated at 1 day after amputation (Rao *et al.*, 2009), and we found another tRNA aminoacylation-related protein CARS was up-regulated at 2 h and 8 h after amputation. In addition, the expression level of SF3B2 for mRNA splicing was increased at 8 h. The results indicate that mRNA processing is a critical for controlling protein synthesis during blastema formation, which was confirmed by a report previously published (Rao *et al.*, 2009).

However, most of ribosomal proteins and translation initiation factors were decreased in expression level, in accordance with the findings that initiation factors was down-regulated at 1 day after amputation of axolotl limb (Rao *et al.*, 2009). Meantime, EIF2 signaling and eIF4 and p70S6K signaling associated with translation was significantly changed at the very early phase of newt limb regeneration. Our data suggest that the differentially expressed proteins involved in the transcriptional and translational machinery are available for whatever protein synthesis is required during newt limb regeneration.

### Cytoskeleton and extracellular matrix

Mononucleate cells from cellularization of myofibers underwent dedifferentiation after amputation of limb (Brockes and Kumar, 2002). A study reported that wound closure in planarians after amputation was facilitated by muscle contraction (Handberg-Thorsager *et al.*, 2008). We found that muscle contraction-related proteins MYH4, MYH6 and MYH13 were up-regulated at 2 h, and MYLK was up-regulated at 8 h. The gradual up-regulation of proteins related to motility, shape and structural integrity was observed at 4 and 7 day after amputation of axolotl limb (Rao *et al.*, 2009), which is consistent with our result that the expression level of microtubule proteins TUBB3, TUBA1C and RMDN1 were increased at 8 h after amputation. TUBB3 was primarily expressed in neurons and might

be involved in neurogenesis and axon guidance and maintenance which were important for limb regeneration. Furthermore, this study found that several signaling pathways associated with the migration of cells into the wound site were significantly enriched by IPA analysis, such as epithelial adherens junction signaling, tight junction signaling, actin cytoskeleton signaling, and ILK signaling, which were also found to participate in regulating the initiation of planarian head regeneration by our previous study (Geng *et al.*, 2015b). These results indicate that epidermal cells might migrate to close the wound through the above mentioned pathways.

With regard to extracellular matrix proteins, we found that the regenerating newt limbs up-regulated fibrinogen and down-regulated type II collagen, which is consistent with the findings that the *Xenopus* and axolotl limbs up-regulated fibrinogen, and down-regulated type II collagen (Rao *et al.*, 2014). The result indicates that the regenerating limb presents a trend toward expression of a less structured matrix.

### Immune response and cell death

Amputation results in tremendous systemic and cellular stress. A major result of cell stress is hypoxia-induced apoptosis (Mescher, 1996). A previous study reported that immediate early response was induced at 2 h post injury of newt heart, and first signals of inflammatory cell recruitment and initiation of cell death happened at 6 h post injury of newt heart (Looso *et al.*, 2013). Similar with this result, our IPA analysis showed that acute phase response signaling was significantly changed at 2 h and 8 h after amputation. Another study reported that cell apoptosis increased in regenerating axolotl limbs immediately after amputation and gradually reduced, and little cell apoptosis was observed on 4 and 7 day, suggesting that cell stress caused by amputation gradually activates anti-apoptosis mechanism during limb regeneration (Rao *et al.*, 2009).

The limb after amputation countered the stress through in-

creasing protein degradation by proteasomes mechanisms, and through the up-regulation expression of chaperones to promote protein folding in the endoplasmic reticulum. Failure to remove the misfolded proteins from the endoplasmic reticulum resulted in apoptosis. IPA analysis showed that endoplasmic reticulum stress was significantly changed at the very early phase of newt limb regeneration, suggesting cell stress response is induced by amputation. Heat shock proteins play crucial roles in the modulation of pathways regulating stem cell activity, regeneration and tissue repair (Isolani *et al.*, 2012). The up-regulation of molecular chaperone HSP90B1 and heat shock proteins HSPA5 and HSPA9 were observed in our study, being consistent with the findings that the level of chaperone genes was increased in the regenerating newt and axolotl limbs (Levesque *et al.*, 2005, Monaghan *et al.*, 2009), *Xenopus laevis* hindlimbs (Pearl *et al.*, 2008). The results indicate that the regenerating limb has some protection against the stress response through the up-regulation expression of chaperones.

It was reported that proteolysis by several proteases is crucial for regulating intestinal regeneration in *Holothuria glaberrima* (Pasten *et al.*, 2012). We found that three of four proteasome proteins were down-regulated by iTRAQ quantitative analysis. The result suggests that the regenerating limb has a degree of resistance to stress, but is inadequate to counter the stress response at the very early phase, leading to a slight increase of apoptosis at the very early phase of newt limb regeneration. Our result was consistent with the findings of Vlaskalin *et al.*, (Vlaskalin *et al.*, 2004) who observed that there was a massive apoptosis in the adult newt forelimbs within the first 3 days post-amputation which did not appear to be present in the axolotl forelimbs, probably due to the fact that cells in the forelimb of the larval axolotl were not fully differentiated.

The vertebrate immune system comprises both adaptive and innate immune cells with distinct functions during the resolution

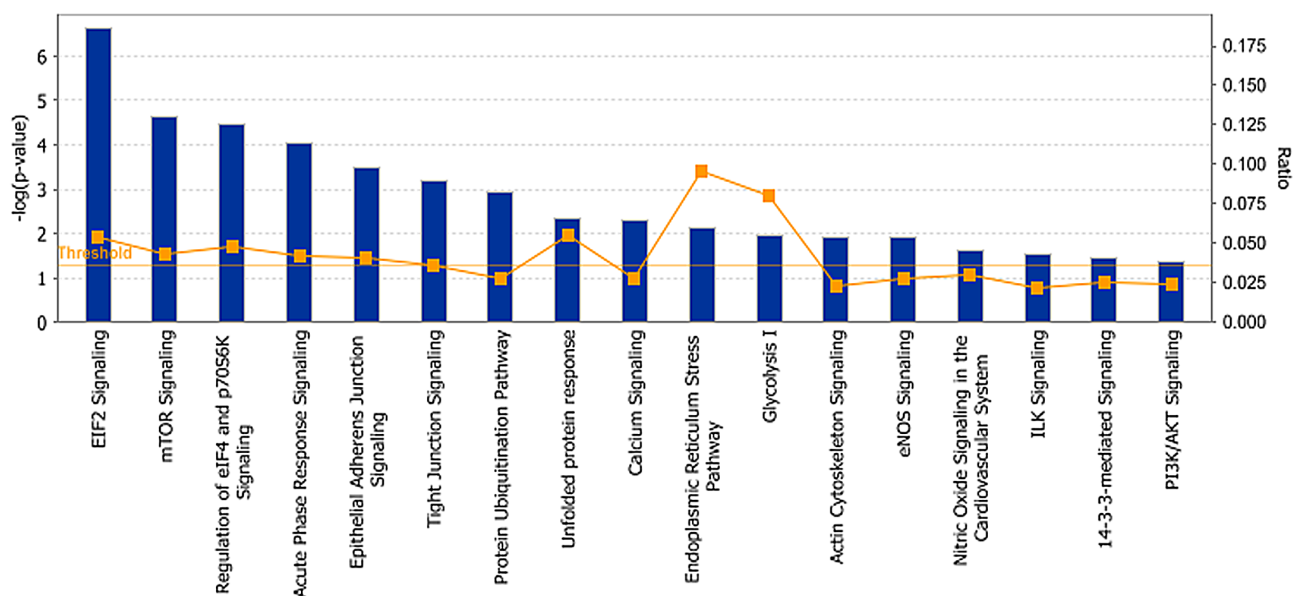


**Fig. 4.** The significantly enriched canonical pathways at the very early phase of newt limb regeneration by IPA software. Each histogram is a particular canonical pathway. The size of the histogram is correlated with increasing overlap significance (Fisher's exact test  $p$ -value). Ratio value represents the number of focus molecules to overall molecules in each canonical pathway.

of inflammation and wound healing after tissue injury (King *et al.*, 2012, Mescher *et al.*, 2013). Recent evidence implicates a requirement for innate immune cells from the myeloid lineage during the early stages of limb regeneration in the Mexican axolotl (Godwin *et al.*, 2013). Previous studies reported that the C3 and C5 proteins were expressed in a complementary fashion during limb regeneration, with C3 being expressed mainly in the blastema and C5 exclusively in the wound epithelium (Del Rio-Tsonis *et al.*, 1998, Kimura *et al.*, 2003). In the present study, the up-regulation expression of complement component C3 was observed in the regenerating newt limb immediately after amputation. These results indicate that C3 is implicated in the dedifferentiation process, and immune response plays important roles in newt limb regeneration.

### Metabolism

It was found that the regenerating tissue exhibited the Warburg effect, and the early blastema relied on anaerobic glycolysis or alternate pathways such as the pentose phosphate shunt and lipid metabolism to maintain ATP production (Naviaux *et al.*, 2009). A recent study reported that carbohydrate regulatory genes played an essential role during *Xenopus* tadpole tail appendage regeneration by stimulating the anabolic pathways required for the reconstruction of a new appendage (Love *et al.*, 2014). Our data showed that glycolysis-related proteins (PGK and GPD1) and fatty acid oxidation-related proteins (ACADM, ACADVL and HADHB) were found to be up-regulated at 8 h after amputation. In addition, several enzymes of tricarboxylic acid cycle, electron transport chain and oxidative phosphorylation were down-regulated in the regenerating newt limb immediately after amputation, including PDHX, NDUFB8, ATP5B and ATP5D. These studies indicate that the limb regeneration immediately after amputation mainly relied on glycolysis and fatty acid oxidation to maintain ATP production, consistent with previous study showing a marked decrease in O<sub>2</sub> usage during early stage of urodele limb regeneration (Rao *et al.*, 2009, Rao *et al.*, 2014).

The iron-binding molecule transferrin is essential for mitosis in the axolotl blastema (Mescher *et al.*, 1997), and was down-regulated in the regenerating newt limb immediately after amputation, indicating that the regenerating limb does not exhibit significant mitosis until the accumulation blastema has formed, whereas mitotic index is as high as 10% in the blastema at 3 day after amputation (Cannata *et al.*, 1992).

### Conclusions

The advanced proteomic technology iTRAQ was utilized to detect the proteomes in the regenerating newt limb at 2 h and 8 h after amputation. In total 152 significantly differentially expressed proteins were identified in our study. Functional annotation found that these proteins were mainly involved in several functional categories including signaling, Ca<sup>2+</sup> binding and translocation, translation, immune response, apoptosis and metabolism. Further IPA analysis showed that several signaling pathways including acute phase response signaling and calcium signaling maybe closely related to the adaptive response immediately after limb amputation. This work provides a basis for further study of regenerative medicine.

## Materials & Methods

### Model preparation of Chinese fire-bellied newt limb regeneration

Chinese fire-bellied newts (*Cynops orientalis*) were collected from Jigong Mountain of Xinyang, Henan province, China. A total of 15 well-grown adult Chinese fire-bellied newts were randomly divided into one control group and two experimental groups with 5 Chinese fire-bellied newts per group. The forelimbs of Chinese fire-bellied newts were amputated in distal portion of stylopod (Humerus) on the right side. The distal tissue with 2 mm was removed at the amputation site and was served as control group. The regenerating tissues with 2 mm in each group were collected at 2 h and 8 h after amputation, respectively. The samples were stored in liquid nitrogen for further use. All experiments were performed in strict accordance with the Animal Protection Law of China.

### Protein extraction and iTRAQ labeling

Protein extraction was performed using a procedure described previously (Geng *et al.*, 2014). Briefly, the frozen regenerating tissues were grinded into fine powder in liquid nitrogen. Then the tissue powder was lysed, and vortexed at 4°C for 1 h. Subsequently, the mixture was centrifuged at 20000 g for 1 h at 4°C. The supernatant was collected and stored at -80°C until further analysis. The concentration of protein was determined using a 2D Quantification kit (GE Healthcare, USA).

A total of 200 µg of each protein sample was denatured, reduced and alkylated as described in the iTRAQ protocol (Applied Biosystems). Each sample was digested with 0.1 µg/µL trypsin solution at 37°C overnight. The digested peptides were dried by vacuum centrifugation. Then the 118, 119 and 121 tags were respectively utilized to label the tryptic peptides from control (0 h), 2 h and 6 h samples. Subsequently, the iTRAQ labeled peptides were pooled and vacuum-dried.

### Strong cation exchange (SCX) chromatography

Strong cation exchange chromatography was performed according to the method previously described (Geng *et al.*, 2015a, Geng *et al.*, 2015b). Briefly, the pooled sample was separated on the Poly-LC strong cation exchange column (4.6 x 100 mm) (5µm, 200Å) using AKTA Purifier 100 (GE Healthcare). The peptides were injected into a liquid SCX chromatography at a flow rate of 0.07 mL/min. Subsequently, the peptides were gradually eluted at a flow rate of 1 mL/min with 10% buffer B (10mM KH<sub>2</sub>PO<sub>4</sub>, 500 mM KCl, 25% acetonitrile, pH 3.0) for 7 min, 10-20% buffer B for 10 min, 20-45% buffer B for 5min, 45-100% buffer B for 5 min. Finally, the system was maintained at 100% buffer B for 8 min. A total of 30 fractions were collected over the gradient, but some were pooled to give a final total of 10 fractions that were desalted using a PepClean C-18 spin column (Sigma, USA), and dried by vacuum centrifugation (Nicholson *et al.*, 2012).

### LC-MS/MS analysis for protein identification

Protein identification by mass spectrometry was performed according to the method previously described (Hsieh *et al.*, 2009). In brief, each fraction was injected into Thermo scientific EASY column (75µm x 100mm, 3µm-C18), and then was separated on Thermo scientific EASY column (2cm x 100µm, 5µm-C18) using Thermo Scientific EASY-nLC 1000 system. Subsequently, the separated samples by capillary high performance liquid chromatography were analyzed by Q-Exactive mass spectrometer (Thermo Fisher Scientific, Waltham, MA, USA) (Geng *et al.*, 2015a, Geng *et al.*, 2015b, Hsieh *et al.*, 2009, Nicholson *et al.*, 2012).

### Data analysis

For peptide data analysis, raw mass data were processed using Proteome Discover 1.4 software and searched against the SwissProt database (March 2013) from Uniprot website (<http://www.uniprot.org>) using Mascot 2.2 (Matrix Science, London, UK). The analysis and search parameters were set as follows: trypsin as the digestion enzyme with allowance for a maximum of two missed cleavage, Carbamidomethyl (C) and iTRAQplex

modification(K and N-terminus) as a fixed modification, Oxidation (M) as a variable modifications, peptide mass tolerance of 20ppm, fragment mass tolerance of 0.1 Da (Geng *et al.*, 2015a, Geng *et al.*, 2015b).

In order to measure the false discovery rate (FDR), the peptide mass spectra datasets were used to search a decoy peptide database. The following filters were used in this study, peptide FDR  $\leq$  0.01 and each protein with at least 2 unique peptides. Expression changes of the identified peptides in the regenerating head fragments were calculated in comparison with the control based on the iTRAQ reporter ion intensities (Unwin *et al.*, 2010). Only unique peptides were utilized to determine protein quantification. In this study, we utilized the frequency distribution histogram to analyze the iTRAQ quantitative data. We firstly calculated the protein ratio by comparing its relative expression level in experimental group to that in normal control group. Then, we calculated a significance score (P-value) for log protein ratios using the method previously published (Cox and Mann, 2008), and the significance score represented the probability of obtaining a log-ratio of at least this magnitude under the null hypothesis that the distribution of log-ratios has normal upper and lower tails. Based on relative quantification and statistical analysis, 1.5-fold change cutoff was selected to categorize proteins as significantly changed, that is, proteins with iTRAQ ratios  $>$  1.5 were considered to be up-regulated, whereas those with iTRAQ ratios  $<$  0.67 were considered to be down-regulated.

### Bioinformatics analysis

In order to characterize the expression patterns of the proteins identified in our quantitative iTRAQ data, Cluster 3.0/TreeView software was used for hierarchical clustering of the differentially expressed proteins as described in detail previously (Geng *et al.*, 2015c).

Gene Ontology (GO) annotation was used to determine the biological processes of the proteins. In addition, the differentially expressed proteins were analyzed by Ingenuity Pathway Analysis (IPA) version 9.0 (Redwood City, CA, <http://www.ingenuity.com>) software for predominant canonical pathways according to the method previously published (Geng *et al.*, 2015a, Geng *et al.*, 2015b). Briefly, a dataset containing these proteins and corresponding extremum of expression values was firstly uploaded into "Dataset Files" of the IPA. Then the proteins were performed by core analysis in IPA. Canonical pathways obtained in this study were identified from the IPA library based on Fisher's Exact Test *P*-value. In this study, pathways with *P*-value $<$ 0.05 were chosen to be predominant at the very early phase of newt limb regeneration.

### Acknowledgements

This work was supported by grants from the National Basic Research 973 Pre-research Program of China (No. 2012CB722304), Natural Science Foundation of China (No. 31572270), the Major Scientific and Technological Projects of Henan (No. 111100910600), the Foundation and Advanced Technology Research Program of Henan (No. 112300413204), and the doctoral Scientific Research Start-up Foundation of Henan Normal University (No. QD14176).

### References

- BROCKES J P and KUMAR A (2002). Plasticity and reprogramming of differentiated cells in amphibian regeneration. *Nat Rev Mol Cell Biol* 3: 566-574.
- BRYANT S V, ENDO T and GARDINER D M (2002). Vertebrate limb regeneration and the origin of limb stem cells. *Int J Dev Biol* 46: 887-896.
- CALDWELL R L, OPALENIK S R, DAVIDSON J M, CAPRIOLI R M and NANNEY L B (2008). Tissue profiling MALDI mass spectrometry reveals prominent calcium-binding proteins in the proteome of regenerative MRL mouse wounds. *Wound Repair Regen* 16: 442-449.
- CANNATA S M, BERNARDINI S and FILONI S (1992). Regenerative responses in cultured hindlimb stumps of larval *Xenopus laevis*. *J Exp Zool* 262: 446-453.
- COX J and MANN M (2008). MaxQuant enables high peptide identification rates, individualized p.p.b.-range mass accuracies and proteome-wide protein quantification. *Nat Biotechnol* 26: 1367-1372.
- DEL RIO-TSONIS K, TSONIS P A, ZARKADIS I K, TSAGAS A G and LAMBRIS J D (1998). Expression of the third component of complement, C3, in regenerating limb blastema cells of urodeles. *J Immunol* 161: 6819-6824.
- GENG X, CHANG C, ZANG X, SUN J, LI P, GUO J and XU C (2016). Integrative proteomic and microRNA analysis of the priming phase during rat liver regeneration. *Gene* 575: 224-232 (doi: 10.1016/j.gene.2015.08.066).
- GENG X, WANG G, QIN Y, ZANG X, LI P, GENG Z, XUE D, DONG Z, MA K, CHEN G *et al.*, (2015b). iTRAQ-Based Quantitative Proteomic Analysis of the Initiation of Head Regeneration in Planarians. *PLoS One* 10: e0132045.
- GENG X, WEI H, SHANG H, ZHOU M, CHEN B, ZHANG F, ZANG X, LI P, SUN J, CHE J *et al.*, (2015c). Proteomic analysis of the skin of Chinese giant salamander (*Andrias davidianus*). *J Proteomics* 119: 196-208.
- GENG X, XU T, NIU Z, ZHOU X, ZHAO L, XIE Z, XUE D, ZHANG F and XU C (2014). Differential proteome analysis of the cell differentiation regulated by BCC, CRH, CXCR4, GnRH, GPCR, IL1 signaling pathways in Chinese fire-bellied newt limb regeneration. *Differentiation* 88: 85-96.
- GLOBUS M, VETHAMANY-GLOBUS S and KESIKA (1987). Control of blastema cell proliferation by possible interplay of calcium and cyclic nucleotides during newt limb regeneration. *Differentiation* 35: 94-99.
- GODWIN J W, PINTO A R and ROSENTHAL N A (2013). Macrophages are required for adult salamander limb regeneration. *Proc Natl Acad Sci U S A* 110: 9415-9420.
- GROW M, NEFF A W, MESCHER A L and KING M W (2006). Global analysis of gene expression in *Xenopus* hindlimbs during stage-dependent complete and incomplete regeneration. *Dev Dyn* 235: 2667-2685.
- HANDBERG-THORSAGER M, FERNANDEZ E and SALO E (2008). Stem cells and regeneration in planarians. *Front Biosci* 13: 6374-6394.
- HSIEH H C, CHEN Y T, LI J M, CHOU T Y, CHANG M F, HUANG S C, TSENG T L, LIU C C and CHEN S F (2009). Protein profilings in mouse liver regeneration after partial hepatectomy using iTRAQ technology. *J Proteome Res* 8: 1004-1013.
- ISOLANI M E, CONTE M, DERI P and BATISTONI R (2012). Stem cell protection mechanisms in planarians: the role of some heat shock genes. *Int J Dev Biol* 56: 127-133.
- ITEN L E and BRYANT S V (1973). Forelimb Regeneration from Different Levels of Amputation in the Newt, *Notophthalmus viridescens*: Length, Rate, and Stages. *Wilhelm Roux' Archiv* 173: 263-282.
- KIMURA Y, MADHAVAN M, CALL M K, SANTIAGO W, TSONIS P A, LAMBRIS J D and DEL RIO-TSONIS K (2003). Expression of complement 3 and complement 5 in newt limb and lens regeneration. *J Immunol* 170: 2331-2339.
- KING M W, NEFF A W and MESCHER A L (2009). Proteomics analysis of regenerating amphibian limbs: changes during the onset of regeneration. *Int J Dev Biol* 53: 955-969.
- KING M W, NEFF A W and MESCHER A L (2012). The developing *Xenopus* limb as a model for studies on the balance between inflammation and regeneration. *Anat Rec (Hoboken)* 295: 1552-1561.
- KUMAR A, GODWIN J W, GATES P B, GARZA-GARCIA A A and BROCKES J P (2007). Molecular basis for the nerve dependence of limb regeneration in an adult vertebrate. *Science* 318: 772-777.
- LEVESQUE M, GUIMOND J C, PILOTE M, LECLERC S, MOLDOVAN F and ROY S (2005). Expression of heat-shock protein 70 during limb development and regeneration in the axolotl. *Dev Dyn* 233: 1525-1534.
- LOOSO M, PREUSSNER J, SOUSOUNIS K, BRUCKSKOTTEN M, MICHEL C S, LIGNELLI E, REINHARDT R, HOFFNER S, KRUGER M, TSONIS P A *et al.*, (2013). A de novo assembly of the newt transcriptome combined with proteomic validation identifies new protein families expressed during tissue regeneration. *Genome Biol* 14: R16.
- LOVE N R, ZIEGLER M, CHEN Y and AMAYA E (2014). Carbohydrate metabolism during vertebrate appendage regeneration: what is its role? How is it regulated?: A postulation that regenerating vertebrate appendages facilitate glycolytic and pentose phosphate pathways to fuel macromolecule biosynthesis. *Bioessays* 36: 27-33.
- MENAA C, DEVLIN R D, REDDY S V, GAZITT Y, CHOI S J and ROODMAN G D (1999). Annexin II increases osteoclast formation by stimulating the proliferation of osteoclast precursors in human marrow cultures. *J Clin Invest* 103: 1605-1613.
- MESCHER A L (1996). The cellular basis of limb regeneration in urodeles. *Int J Dev Biol* 40: 785-795.
- MESCHER A L, CONNELL E, HSU C, PATEL C and OVERTON B (1997). Transfer-

- rin is necessary and sufficient for the neural effect on growth in amphibian limb regeneration blastemas. *Dev Growth Differ* 39: 677-684.
- MESCHER A L, NEFF A W and KING M W (2013). Changes in the inflammatory response to injury and its resolution during the loss of regenerative capacity in developing *Xenopus* limbs. *PLoS One* 8: e80477.
- MONAGHAN JR, EPP L G, PUTTAS, PAGE R B, WALKER J A, BEACHY C K, ZHU W, PAO G M, VERMA I M, HUNTER T *et al.*, (2009). Microarray and cDNA sequence analysis of transcription during nerve-dependent limb regeneration. *BMC Biol* 7: 1.
- MORRISON J I, LOOF S, HE P and SIMON A (2006). Salamander limb regeneration involves the activation of a multipotent skeletal muscle satellite cell population. *J Cell Biol* 172: 433-440.
- MORZLOCK F V and STOCUM D L (1971). Patterns of RNA synthesis in regenerating limbs of the adult newt, *Triturus viridescens*. *Dev Biol* 24: 106-118.
- NAVIAUX R K, LE T P, BEDELBAEVA K, LEFEROVICH J, GOUREVITCH D, SACHADYN P, ZHANG X M, CLARK L and HEBER-KATZ E (2009). Retained features of embryonic metabolism in the adult MRL mouse. *Mol Genet Metab* 96: 133-144.
- NICHOLSON J, NEELAGANDAN K, HUART A S, BALL K, MOLLOY M P and HUPP T (2012). An iTRAQ proteomics screen reveals the effects of the MDM2 binding ligand Nutlin-3 on cellular proteostasis. *J Proteome Res* 11: 5464-5478.
- NYE H L, CAMERON J A, CHERNOFF E A and STOCUM D L (2003). Regeneration of the urodele limb: a review. *Dev Dyn* 226: 280-294.
- PASTEN C, ROSA R, ORTIZ S, GONZALEZ S and GARCIA-ARRARAS J E (2012). Characterization of proteolytic activities during intestinal regeneration of the sea cucumber, *Holothuria glaberrima*. *Int J Dev Biol* 56: 681-691.
- PEARL E J, BARKER D, DAY R C and BECK C W (2008). Identification of genes associated with regenerative success of *Xenopus laevis* hindlimbs. *BMC Dev Biol* 8: 66.
- RAO N, JHAMB D, MILNER D J, LI B, SONG F, WANG M, VOSS S R, PALAKAL M, KING M W, SARANJAMI B *et al.*, (2009). Proteomic analysis of blastema formation in regenerating axolotl limbs. *BMC Biol* 7: 83.
- RAO N, SONG F, JHAMB D, WANG M, MILNER D J, PRICE N M, BELECKY-ADAMS T L, PALAKAL M J, CAMERON J A, LI B *et al.*, (2014). Proteomic analysis of fibroblastema formation in regenerating hind limbs of *Xenopus laevis* froglets and comparison to axolotl. *BMC Dev Biol* 14: 32.
- SEI Y, GALLAGHER K L and BASILE A S (1999). Skeletal muscle type ryanodine receptor is involved in calcium signaling in human B lymphocytes. *J Biol Chem* 274: 5995-6002.
- TAKAI Y, SASAKI T and MATOZAKI T (2001). Small GTP-binding proteins. *Physiol Rev* 81: 153-208.
- TSONIS P A (1993). A comparative two-dimensional gel protein database of the intact and regenerating newt limbs. *Electrophoresis* 14: 148-156.
- TSONIS P A, MESCHER A L and DEL RIO-TSONIS K (1992). Protein synthesis in the newt regenerating limb. Comparative two-dimensional PAGE, computer analysis and protein sequencing. *Biochem J* 281: 665-668.
- UNWIN R D, GRIFFITHS J R and WHETTON A D (2010). Simultaneous analysis of relative protein expression levels across multiple samples using iTRAQ isobaric tags with 2D nano LC-MS/MS. *Nat Protoc* 5: 1574-1582.
- VASCOTTO S G, BEUG S, LIVERSAGE R A and TSILFIDIS C (2005). Identification of cDNAs associated with late dedifferentiation in adult newt forelimb regeneration. *Dev Dyn* 233: 347-355.
- VLASKALIN T, WONG C J and TSILFIDIS C (2004). Growth and apoptosis during larval forelimb development and adult forelimb regeneration in the newt (*Notophthalmus viridescens*). *Dev Genes Evol* 214: 423-431.
- VORPAHL M, SCHONHOFER-MERL S, MICHAELIS C, FLOTHO A, MELCHIOR F and WESSELY R (2014). The Ran GTPase-activating protein (RanGAP1) is critically involved in smooth muscle cell differentiation, proliferation and migration following vascular injury: implications for neointima formation and restenosis. *PLoS One* 9: e101519.
- WU C H, TSAI M H, HO C C, CHEN C Y and LEE H S (2013). De novo transcriptome sequencing of axolotl blastema for identification of differentially expressed genes during limb regeneration. *BMC Genomics* 14: 434.

**Further Related Reading, published previously in the *Int. J. Dev. Biol.***

**Characterization of proteolytic activities during intestinal regeneration of the sea cucumber, *Holothuria glaberrima***

Consuelo Pasten, Rey Rosa, Stephanie Ortiz, Sebastián González and José E. García-Arrarás

*Int. J. Dev. Biol.* (2012) 56: 681-691

<http://dx.doi.org/10.1387/ijdb.113473cp>

**Stem cell protection mechanisms in planarians: the role of some heat shock genes**

Maria-Emilia Isolani, Maria Conte, Paolo Deri and Renata Batistoni

*Int. J. Dev. Biol.* (2012) 56: 127-133

<http://dx.doi.org/10.1387/ijdb.113432mi>

**Proteomics analysis of regenerating amphibian limbs: changes during the onset of regeneration**

Michael W. King, Anton W. Neff and Anthony L. Mescher

*Int. J. Dev. Biol.* (2009) 53: 955-969

<http://dx.doi.org/10.1387/ijdb.082719mk>

**Vertebrate limb regeneration and the origin of limb stem cells**

Susan V Bryant, Tetsuya Endo and David M Gardiner

*Int. J. Dev. Biol.* (2002) 46: 887-896

**The cellular basis of limb regeneration in urodeles**

A L Mescher

*Int. J. Dev. Biol.* (1996) 40: 785-795

<http://www.ijdb.ehu.es/web/paper/8877452>

**5 yr ISI Impact Factor (2013) = 2.879**

